Biometrics, 2025, 81(3), ujaf081
https://doi.org/10.1093/biomtc/ujaf081
Biometric Practice

OXFORD

Inference on age-specific fertility in ecology and evolution. Learning from other disciplines and improving the state of the art

Fernando Colchero [1,2,*]

[1]Department of Primate Behavior and Evolution, Max Planck Institute for Evolutionary Anthropology, 04103, Leipzig, Germany, [2]Department of Mathematics and Computer Science, University of Southern Denmark, 5230, Odense, Denmark

[*]Corresponding author: Fernando Colchero, Department of Primate Behavior and Evolution, Max Planck Institute for Evolutionary Anthropology (MPI-EVA), Deutscher Platz 6, 04103 Leipzig, Germany (fernando_colchero@eva.mpg.de).

ABSTRACT

Despite the importance of age-specific fertility for ecology and evolution, the methods for modeling and inference have proven considerably limited. However, other disciplines have long focused on exploring and developing a vast number of models. Here, I provide an overview of the different models proposed since the 1940s by formal demographers, statisticians, and social scientists, most of which are unknown to the ecological and evolutionary communities. I describe how these fall into 2 main categories, namely polynomials and those based on probability density functions. I discuss their merits in terms of their overall behavior and how well they represent the different stages of fertility. Despite many alternative models, inference on age-specific fertility has usually been limited to simple least squares. Although this might be sufficient for human data, I hope to demonstrate that inference requires more sophisticated approaches for ecological and evolutionary datasets. To illustrate how inference and model choice can be achieved on different types of typical ecological and evolutionary data, I present the new R package Bayesian Fertility Trajectory Analysis, which I apply to published aggregated data for lions and baboons. I then conduct a simulation study to test its performance on individual-level data. I show that appropriate inference and model selection can be achieved even when a small number of parents are followed.

KEYWORDS: age-specific fertility; Bayesian inference; compound Poisson process; demography; nonhomogeneous Poisson process.

1 INTRODUCTION

Fertility is one of the fundamental building blocks of demography and, therefore, of any discipline derived from it, such as population ecology (Colchero et al., 2019) or evolutionary studies that focus on population-level processes (Lowe et al., 2017). Despite its importance, it has not garnered the same attention as survival, for which the statistical tools available to ecologists and evolutionary biologists are vast. Therefore, this contribution aims to provide an overview of the parametric models available to estimate age-specific fertility developed in other disciplines and how estimation can be adapted to the different types of datasets from species other than humans for studies on ecology and evolutionary biology.

Notably, the review of the models available focuses on fertility and not fecundity. Although these terms are often used interchangeably, it is important to stress that fertility and fecundity represent 2 related but different aspects of reproduction. Starting when individuals reach sexual maturity, fecundity is the potential of an individual to reproduce, while fertility is the number of offspring produced by individuals in the population, and it is assumed to start at the first sexual intercourse. Therefore, fertility focuses on the number of life births and, what is commonly known as the fertility rate, is often measured as the average number of offspring produced per sexually mature individuals in the population (for an in depth review see Bradshaw and McMahon, 2008).

In addition, this review does not focus on models for reproductive cessation (Packer et al., 1998; Alberts et al., 2013), albeit some of the models discussed in the following sections can account for it. Similarly, I will not review models that have been developed specifically for human populations, such as those proposed by Brass (1968), Coale and Trussell (1974), or Gupta and Pasupuleti (2013), and may not be easily generalized to other species.

In the following sections, I will first present several of the available age-specific fertility models proposed in different disciplines (eg, demography, social sciences, applied statistics), distinguishing between the type of models (ie, polynomial or distributional). I then discuss how the standard practice for inference on these models is generally inappropriate for typical datasets in ecology and evolution and provide an overview of the most common types of datasets, namely aggregated, individual-level data with discrete ages for seasonal breeders, and individual-level data with continuous ages and variable interbirth intervals (IBIs). In this section, I propose how likelihood functions can be specified for each type of data. I follow by presenting the R package BaFTA

Received: January 18, 2024; Revised: May 2, 2025; Accepted: June 12, 2025

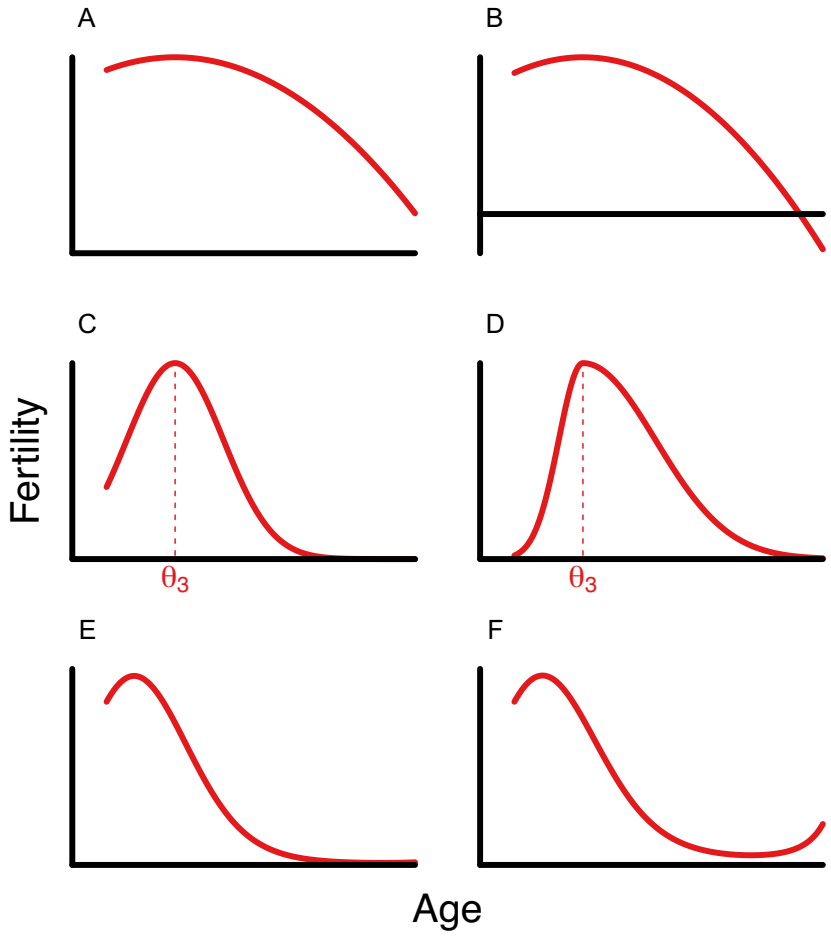

FIGURE 1 Age-specific fertility models based on the quadratic model. (A) Basic quadratic model as in Equation (1); (B) basic quadratic model not conforming to the definition of function g; (C) exponential quadratic model as in Equation (2); (D) model by Peristera and Kostaki (2007) solving the issue of symmetry around θ_3; (E) cubic splines as models of age-specific fertility as depicted in Equation (5) without anomalous behavior; and (F) cubic splines with anomalous behavior at the end of the reproductive life course.

for Bayesian Fertility Trajectory Analysis, which facilitates making inferences on age-specific fertility for all 3 types of data. I illustrate its use both on published aggregated data and simulated data for inference on individual-level data with continuous ages. I conclude by showing the results of simulation studies where I test the performance of the package on simulated data.

2 AGE-SPECIFIC FERTILITY MODELS

2.1 General considerations

Parametric models of age-specific fertility require defining a continuous and smooth parametric function $g : \mathbb{R}_{\geq 0} \rightarrow \mathbb{R}_{\geq 0}$, where $\mathbb{R}_{\geq 0} = \{x \in \mathbb{R} | x \geq 0\}$, for the expected number of offspring produced per female at age $x \geq 0$. As the definition shows, the function g needs to be continuous in $\mathbb{R}_{\geq 0}$ and requires positive real ages as inputs, while it cannot produce negative expected offspring. Statistical inference is needed for estimation of the vector of fertility parameters $\boldsymbol{\theta} \in \mathbb{R}^p$ of length p, which determine the form of function g, and therefore provide information on the population's age-specific fertility.

Note that, in the following sections, for simplicity I define ages as $x = \text{age} - \alpha$, where $\alpha \geq 0$ is the minimum age at maturity, unless otherwise indicated. I also define $\omega > \alpha$ as the maximum age or the age of reproductive cessation. Furthermore, it should be assumed that the vector of fertility parameters is $\boldsymbol{\theta}^\top = [\theta_1, \ldots, \theta_p]$ where θ_j for $j = 1, 2, \ldots, p$ are scalar fertility parameters to be estimated.

2.2 Polynomials and cubic splines

The most common model for age-specific fertility used in ecology and evolution is the quadratic model (McCleery et al., 2008; Sharp and Clutton-Brock, 2010; Dugdale et al., 2011), often parametrized as

$$g(x|\boldsymbol{\theta}) = \theta_1 - \theta_2(x - \theta_3)^2, \tag{1}$$

where $\theta_1, \theta_2 > 0$ and $\theta_3 \geq 0$ are fertility parameters to be estimated and, as defined above, $x \geq 0$ is adult age (Figure 1A). An advantage of this implementation is that the parameters have a clear interpretation, namely, θ_1 provides the level of maximum fertility, θ_2 controls the rate of increase and decrease in fertility around θ_3 which corresponds to the age of maximum fertility. Although quite appealing, this implementation can be problematic since it does not follow the proper definition of function g provided in the previous section, namely that the range of the

function is not bound within $\mathbb{R}_{\geq 0}$, but it can produce negative values when $\theta_2(x-\theta_3)^2 > \theta_1$, which may occur at the boundaries of the age range (Figure 1B).

An alternative implementation of the quadratic model in Equation (1) that resolves the issue above is

$$g(x|\boldsymbol{\theta}) = \theta_1 \exp\left[-\theta_2(x-\theta_3)^2\right]. \tag{2}$$

Here, the interpretation of the parameters remains as for Equation (1), but now the model conforms to the definition of function g (Figure 1C). However, despite the clear link between the parameters in Equations (1) and (2) and biological aspects of fertility, these models still bear important limitations. Specifically, they are both symmetric around θ_3, thus the initial rate of increase in fertility is equivalent to the rate of decline after the age of maximum fertility. It is well known that the processes at play during these 2 periods of the reproductive life course are considerably different, whereby the initial increase in fertility is due in part to the gradual onset of reproductive maturity, while the subsequent decline in fertility is due to processes related to reproductive senescence, the progressive decline in reproductive capacity with age (Lemaître et al., 2020).

As an alternative to circumvent this limitation, the model by Peristera and Kostaki (2007) provides a small but significant change to Equation (2), given by

$$g(x|\boldsymbol{\theta}) = \theta_1 \exp\left[-\left(\frac{x-\theta_3}{\theta_{21}^{\xi}\,\theta_{22}^{(1-\xi)}}\right)^2\right], \tag{3}$$

where $\theta_1 > 0, \theta_3 \geq 0$ and $\theta_{21}, \theta_{22} > 0$, and where $\xi \in \{0, 1\}$ is an indicator such that $\xi = 1$ if $x \leq \theta_3$ and $\xi = 0$ if $x > \theta_3$. This more flexible implementation bears the same interpretation of θ_1 and θ_3 as for Equations (1) and (2), but with the difference that now $1/\theta_{21}$ controls the rate of increase in fertility before the age at maximum fertility, θ_3, and $1/\theta_{22}$ drives the rate of fertility decline after this age (Figure 1D).

Similarly, in order to circumvent the limitation of symmetry around θ_3, Muller et al. (2020) and Colchero et al. (2021) proposed the function

$$g(x|\boldsymbol{\theta}) = \theta_1 \exp\left[\theta_2(x-\theta_3)^2 + \theta_4/(x+1)\right], \tag{4}$$

where, as in Equation (2), $\theta_1, \theta_2 > 0$ and $\theta_3 \geq 0$ and $\theta_4 \in \mathbb{R}$. Thus, the quadratic function in Equation (2) is a special case of Equation (4) where $\theta_4 = 0$. The authors show that this model provides a better fit than the quadratic model in Equation (2) to data from hunter gatherers, chimpanzees and gorillas.

Alternatively, polynomials of higher degree have been proposed to reduce the issues of symmetry in Equations (1) and (2) (Hoem et al., 1981; Islam, 2011). However, using higher order polynomials does not conform to the definition of function g unless they are transformed, for instance, as in Equation (2). In addition, increasing the order of the polynomial risks producing anomalous behaviors at the bounds of the age range (eg, artificial increases in fertility at older ages).

Similar to higher order polynomials, cubic splines have also been proposed to model age-specific fertility (Hoem et al., 1981; Schmertmann, 2003; Beer, 2011). These are parametrized as

$$g(x|\boldsymbol{\theta}) = \sum_{k=0}^{3} \theta_{1,k} x^k + \sum_{k=1}^{3} \theta_{2,k}(x-\theta_{3,k})^3 \theta_{4,k}, \tag{5}$$

where $\theta_{1,i}$ and $\theta_{2,j}$ for $i = 0, 1, 2, 3$ and $j = 1, 2, 3$ are polynomial and spline coefficients, $\theta_{3,k}$ are spline knots, and $\theta_{4,k}$ are indicators that take $\theta_{4,k} = 1$ if $x > \theta_{3,k}$ and 0 otherwise (Figure 1E). Although the model in Equation (5) has been shown to produce good fits to human fertility data (Hoem et al., 1981), it requires up to 10 parameters, risking over parametrization. In addition, it bears the same limitations as higher degree polynomials as described above (Figure 1F).

2.3 Unimodal distributional models

A common and often preferred alternative to polynomials and cubic splines are models for which the fertility function is specified as

$$g(x|\boldsymbol{\theta}) = \theta_0 f(x|\boldsymbol{\theta}_1), \tag{6}$$

where $\boldsymbol{\theta}^\top = [\theta_0, \boldsymbol{\theta}_1^\top]$, and $\theta_0 > 0$ is a parameter that represents the total fertility rate (commonly noted as R, Hoem et al. 1981), while function $f : \mathbb{R}_{\geq 0} \to \mathbb{R}_{\geq 0}$ is a continuous parametric probability density function (PDF) with parameter vector $\boldsymbol{\theta}_1 \in \mathbb{R}^k$ of length $k = p - 1$.

Although the density f can be interpreted as the distribution of the parent's age of a randomly selected birth, it is meant to provide a flexible shape for the fertility function that abides by the definition of function g. Using density f therefore requires the scaling parameter θ_0, which, as we mentioned above, is equivalent to the average total fertility since $\int_0^\infty \theta_0 f(x|\boldsymbol{\theta})dx = \theta_0$.

Notably, some of the common summary statistics of the PDFs for function f can be used to calculate useful reproduction measures, such as the mode to obtain the age at maximum fertility, using upper and lower quantiles to measure the duration of effective breeding (Clutton-Brock and Isvaran, 2007) or as the basis for the estimation of post-reproductive representation (Levitis and Lackey, 2011).

In the early 1940s, Hadwiger (1940) proposed the first distributional model, given by

$$g(x|\boldsymbol{\theta}) = \frac{\theta_1\theta_2}{\theta_3}\left(\frac{\theta_3}{x}\right)^{3/2} \exp\left[-\theta_2^2\left(\frac{\theta_3}{x} + \frac{x}{\theta_3} - 2\right)\right], \quad \text{for } x > 0 \tag{7}$$

where $\theta_j > 0$ for $j = 1, 2, 3$ (Figure 2A). As described by Hoem et al. (1981), the model is derived from the inverse Gaussian distribution, where the parameters in $\boldsymbol{\theta}$ have no direct interpretation. However, they show that, after some transformations, the parameters can be reformulated in terms of θ_0 and the distribution's mode, mean and variance.

In addition, Hoem et al. (1981) proposed the use of other distributions for function f in Equation (6) such as the gamma density, given by

$$f(x|\boldsymbol{\theta}_1) = \frac{1}{\Gamma(\theta_1)\theta_2^{\theta_1}} x^{\theta_1 - 1} e^{x/\theta_2}, \quad \text{for } x \geq 0, \tag{8}$$

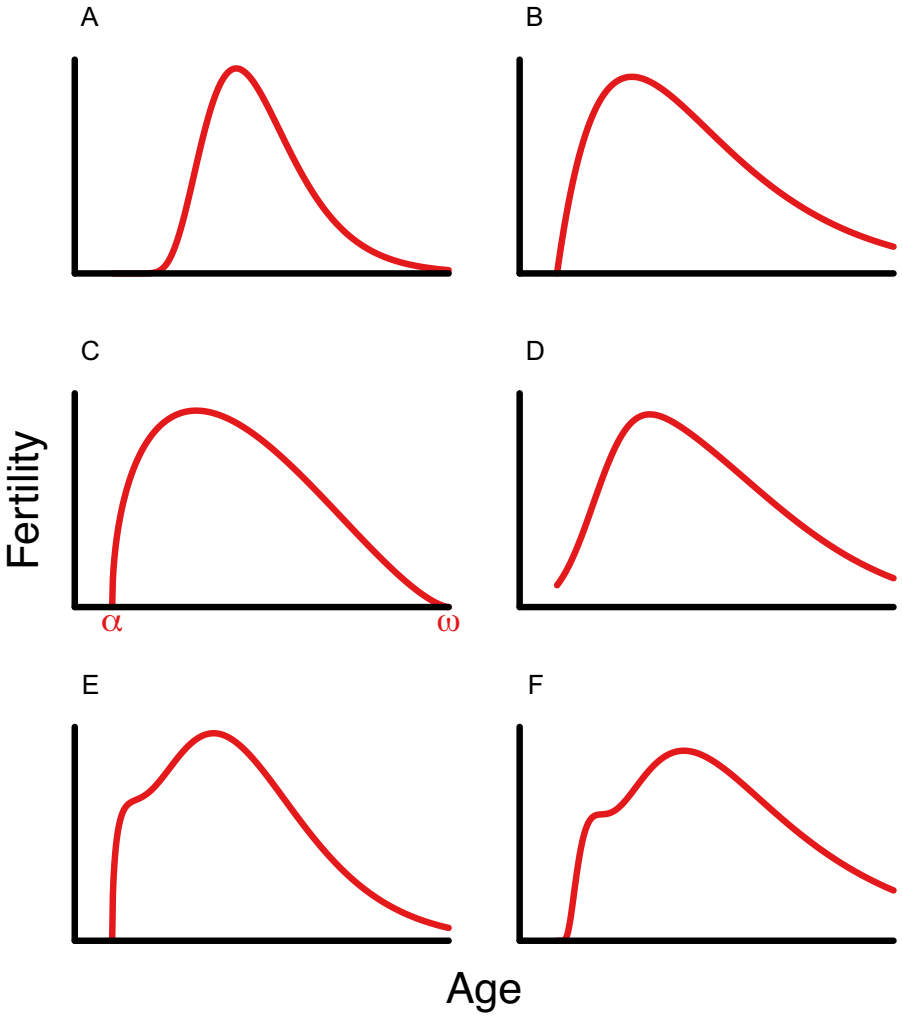

FIGURE 2 Density based models of fertility: (A) Hadwiger (Hadwiger, 1940); (B) gamma (Hoem et al., 1981); (C) 4 parameter beta (Hoem et al., 1981); (D) skew normal (Mazzuco and Scarpa, 2011; 2015); (E) gamma mixture (Hoem et al., 1981); and (F) Hadwiger mixture (Chandola et al., 1999).

where $\theta_1, \theta_2 > 0$ are the shape and scale parameters, respectively, and $\Gamma(\theta_1)$ is the gamma function (Figure 2B). Another distribution proposed by Hoem et al. (1981) is the 4 parameter beta density, with alternative parametrization given by

$$f(x|\boldsymbol{\theta}_1) = \frac{(x-\alpha)^{\theta_1-1}(\omega-x)^{\theta_2-1}}{(\omega-\alpha)^{\theta_1+\theta_2-1}B(\theta_1,\theta_2)}, \quad \text{for } \alpha \leq x \leq \omega, \tag{9}$$

where $\theta_1, \theta_2 > 0$ and $B(\theta_1, \theta_2)$ is the beta function (Figure 2C). Here, θ_1 and θ_2 are the shape parameters of the density, and, as defined previously, α and ω are the lower and upper bounds of the age range. In other words, $x \in [\alpha, \omega]$ and thus α is the minimum age of first birth or sexual maturity, and ω is the maximum age of fertility or lifespan. As it can be inferred, this model is well suited for species for which reproductive cessation is known to occur, such as humans, elephants, or killer whales (Ellis et al., 2018).

Another alternative model is the skew-normal model (Figure 2D) originally described by Azzalini (1985) and later proposed by Mazzuco and Scarpa (2011; 2015) for fertility estimation, given by

$$f(x|\boldsymbol{\theta}_1) = 2\theta_1^{-1}\phi\left(\frac{x-\theta_3}{\theta_1}\right)\Phi\left[\theta_2\left(\frac{x-\theta_3}{\theta_1}\right)\right], \tag{10}$$

where ϕ is the PDF and Φ the cumulative distribution function (CDF) of the standard normal distribution, $\theta_1, \theta_2 > 0$ are scale and shape parameters, respectively, and $\theta_3 \in \mathbb{R}$ is a location parameter.

2.4 Bimodal distributional models

The models in Equations (7)–(10) have been appropriately fitted to unimodal fertility curves such as the 1965 or 1994 Danish fertility, as well as the 1994 French, Austrian, and Swedish fertility curves (Hoem et al., 1981; Chandola et al., 1999). However, these models could not reproduce curves that had excess fertility at younger ages, seemingly associated with differences between non-marital and marital fertility (Chandola et al., 1999), which produced bimodal fertility curves (Chandola et al., 1999; Peristera and Kostaki, 2007; Bermúdez et al., 2012; Mazzuco and Scarpa, 2015). A simple solution was then to use mixture

models, which combine 2 distributions as

$$g(x|\boldsymbol{\theta}) = \theta_0 \left[\theta_1 f_1(x|\boldsymbol{\theta}_1) + (1-\theta_1) f_2(x|\boldsymbol{\theta}_2)\right], \quad (11)$$

where $\theta_1 \in [0, 1]$ is the mixture parameter and $f_1(x|\boldsymbol{\theta}_1)$ and $f_2(x|\boldsymbol{\theta}_2)$ are 2 distributions with parameter vectors $\boldsymbol{\theta}_1$ and $\boldsymbol{\theta}_2$, where $\boldsymbol{\theta}^\top = [\theta_0, \theta_1, \boldsymbol{\theta}_1^\top, \boldsymbol{\theta}_2^\top]$. For instance, Hoem et al. (1981) proposed extending the gamma model in Equation (8) according to Equation (11) (Figure 2E). Following this framework, Chandola et al. (1999) proposed a Hadwiger mixture model (Figure 2F) given by

$$\begin{aligned} g(x|\boldsymbol{\theta}) = \theta_0 \Bigg\{ & \theta_1 \left(\frac{\theta_3}{\theta_4}\right) \left(\frac{\theta_4}{x}\right)^{3/2} \exp\left[-\theta_3^2 \left(\frac{\theta_4}{x} + \frac{x}{\theta_4} - 2\right)\right] \\ & + (1-\theta_1) \left(\frac{\theta_5}{\theta_6}\right) \left(\frac{\theta_6}{x}\right)^{3/2} \\ & \times \exp\left[-\theta_5^2 \left(\frac{\theta_6}{x} + \frac{x}{\theta_6} - 2\right)\right]\Bigg\}, \end{aligned} \quad (12)$$

with $\theta_3, \ldots, \theta_6 > 0$. Other mixture models include the scaled Weibull mixture proposed by Bermúdez et al. (2012).

Although their model is not in essence distributional, Peristera and Kostaki (2007) proposed a mixture of the model in Equation (3) given by

$$\begin{aligned} g(x|\boldsymbol{\theta}) = & \theta_1 \exp\left[-\left(\frac{x-\theta_3}{\theta_{21}^{\varepsilon_1}\theta_{22}^{(1-\varepsilon_1)}}\right)^2\right] \\ & + \theta_4 \exp\left[-\left(\frac{x-\theta_6}{\theta_{51}^{\varepsilon_2}\theta_{52}^{(1-\varepsilon_2)}}\right)^2\right], \end{aligned} \quad (13)$$

where the parameters in $\boldsymbol{\theta}$ follow the same constraints as for Equation (3).

Other notable models proposed to account for bimodal fertility are based on skew- symmetric distributions (Azzalini, 1985; Ma and Genton, 2004), with general form given by

$$g(x|\boldsymbol{\theta}) = \theta_0\, 2 f(x) G[w(x)], \quad (14)$$

where $f : \mathbb{R}_{\geq 0} \to \mathbb{R}_{\geq 0}$ is any PDF symmetric about the mean, $G : \mathbb{R}_{\geq 0} \to [0, 1]$ is a CDF with symmetric PDF, and w is commonly an odd polynomial that acts as the skewing function. Notably, 2 skew-symmetric models have been used for modeling fertility, the first being the skew-symmetric based on standard normal distributions proposed by Mazzuco and Scarpa (2011; 2015), given by

$$\begin{aligned} g(x|\boldsymbol{\theta}) = & \theta_0\, 2\theta_1^{-1} \phi\left(\frac{x-\theta_3}{\theta_1}\right) \Phi \\ & \times \left[\theta_2 \left(\frac{x-\theta_3}{\theta_1}\right) + \theta_4 \left(\frac{x-\theta_3}{\theta_1}\right)^3\right], \end{aligned} \quad (15)$$

where parameters $\theta_1, \ldots, \theta_3$ are as for Equation (10), and $\theta_4 \in \mathbb{R}$ controls whether the distribution is bimodal (Ma and Genton, 2004).

Similarly, Asili et al. (2014) proposed the skew-logistic model which, after some transformations to make it comparable to the skew-symmetric model, it becomes

$$g(x|\boldsymbol{\theta}) = \theta_0\, 2\theta_1^{-1} \frac{e^{-(x-\theta_3)/\theta_1}}{\left(1+e^{-(x-\theta_3)/\theta_1}\right)^2 \left\{1 + e^{-\theta_2[(x-\theta_3)/\theta_1] - \theta_4[(x-\theta_3)/\theta_1]^3}\right\}}. \quad (16)$$

As for the skew-symmetric, $\theta_1, \theta_2 > 0$ are scale and shape parameters, respectively, $\theta_3 \in \mathbb{R}$ is a location parameter, and $\theta_4 \in \mathbb{R}$ makes the distribution bimodal, particularly when $\theta_4 < 0$. Note that both models in Equations (15) and (16) can produce a similar odd behavior at the oldest ages as the higher order polynomial and cubic spline models (eg, Figure 1F).

3 DATA TYPES AND CORRESPONDING LIKELIHOOD FUNCTIONS

The models described in Section 2 are, in most cases, fitted by means of non-linear least squares on average age-specific fertilities (Hoem et al., 1981; Chandola et al., 1999; Mazzuco and Scarpa, 2011; 2015). By using least squares instead of likelihood-based approaches, we ignore important sources of uncertainty, such as the number of individuals that contributed to the estimation at every age. Although this may not seem an important issue when analyzing human fertility data, it can greatly affect proper estimation for species and populations with limited data.

Importantly, inference needs to consider not only the type of data as determined by the way they were collected (ie, aggregated vs individual level) but also biological processes, such as whether reproduction occurs seasonally or year-round. In addition, the ultimate aim of estimating fertility should play a role. For instance, If the purpose is to model population dynamics by means of, say, matrix projection models (Caswell, 2019), then it is sufficient to estimate fertility as the average number of offspring produced by all alive adults per age interval $[x, x+1)$. However, suppose we are interested in estimating the average number of offspring produced per reproductive event at a given age x in non-seasonal species and with IBIs different from unity. In that case, this measure of fertility will differ from the average number of offspring produced per age interval. Let $g_d(x)$ be the fertility estimated within discrete age intervals, and let $g_c(x)$ be the fertility per reproductive event (ie, continuous time). If within an age interval $[x, x+1)$ individuals can reproduce on average $\tau > 0$ times, then the fertility estimated from discrete ages, $g_d(x)$, can be approximated as

$$g_d(x) \approx \tau g_c\left(x + \frac{1}{2}\right). \quad (17)$$

3.1 Individual level data with seasonal reproduction

Data on age-specific fertility often consists of individual-level information, where individuals and their reproductive output are followed for some time. In this case, datasets consist of repeated records per parent at different ages in discrete time and the number of offspring they produced at each age.

Here, we can define the nonhomogeneous Poisson process $\{N(x), x \geq 0\}$ with intensity function $\lambda(x)$, where $N(x)$ are the cumulative number of offspring produced by a given individual up to age x. At a given discrete age interval $[x, x+1)$, we can

define the random variable for an average individual as

$$Y_x = N(x+1) - N(x) \sim \text{Pois}[\Lambda(x+1) - \Lambda(x)], \tag{18}$$

where

$$\Lambda(x) = \int_0^x \lambda(t)dt. \tag{19}$$

For age intervals of 1 year, $\lambda(x)$ can be calculated at the midpoint of the interval $[x, x+1)$ such that

$$\int_x^{x+1} \lambda(t)dt = \Lambda(x+1) - \Lambda(x) = \lambda\left(x + \frac{1}{2}\right) + \varepsilon_x, \tag{20}$$

where, based on the error of the midpoint rule, $\varepsilon_x \leq \frac{K}{24}$ and $K \geq |\lambda''(t)|$ for all $t \in [x, x+1]$. Given that g is a concave function of age, we can therefore assume that the error ε_x is negligible.

The random variable Y_x in Equation (18) represents the number of offspring produced within the age interval $[x, x+1)$ by an average individual. However, given that individuals differ in their ability to reproduce, a hierarchical model is more appropriate (Muller et al., 2020; Colchero et al., 2021). Here, we define the conditional random variable

$$\begin{aligned} Y_{i,x}|U_i &\sim \text{Pois}[\lambda(x, U_i)] \\ U_i &\sim Ga(\gamma, \gamma), \end{aligned} \tag{21}$$

where $\gamma > 0$, with observations $y_{i,x} \in \mathbb{N}_{\geq 0}$, $U_1, \ldots, U_{n_x}$ are i.i.d. random variables variable with $E(U_i) = 1$ for $i = 1, 2, \ldots, n_x$ where n_x is the number of parents at age x, and $g : \mathbb{R}_{\geq 0} \to \mathbb{R}_{\geq 0}$ is a $k \geq 2$ times differentiable smooth concave function. The conditional expectation is then given by

$$E(Y_{i,x}|U_i) = \lambda(x, U_i) = U_i g(x), \tag{22}$$

evaluated at $x + 1/2$.

The random variable $Y_{i,x}$ is marginally distributed as $Y_{i,x} \sim \text{NB}[\gamma, \gamma/(g(x)+\gamma)]$, with marginal probability mass function given by

$$f_Y(y_{i,x}) = \frac{\Gamma(y_{i,x}+\gamma)}{\Gamma(\gamma)y_{i,x}!}\left(\frac{\gamma}{g(x)+\gamma}\right)^{\gamma}\left(\frac{g(x)}{g(x)+\gamma}\right)^{y_{i,x}} \quad \text{for } y_{i,x} \in \mathbb{N}_{\geq 0}, \tag{23}$$

where $\text{E}[Y_{i,x}] = g(x)$ and $\text{Var}[Y_{i,x}] = g(x)[(g(x)+\gamma)/\gamma]$. The likelihood function is then given by

$$\mathcal{L}(\boldsymbol{y}|\boldsymbol{\theta}, \sigma^2) = \prod_{i=1}^{n}\prod_{x\in E_i}\frac{\Gamma(y_{i,x}+\gamma)}{\Gamma(\gamma)y_{i,x}!}\left(\frac{\gamma}{g(x)+\gamma}\right)^{\gamma} \times \left(\frac{g(x)}{g(x)+\gamma}\right)^{y_{i,x}}, \tag{24}$$

where E_i is the set of ages at which individual i was known to be present.

An alternative implementation, as in Colchero et al. (2021) and Muller et al. (2020) is given by

$$\begin{aligned} Y_{i,x}|U_i &\sim \text{Pois}[\lambda(x, U_i)] \\ U_i &\sim N(0, \sigma^2) \end{aligned} \tag{25}$$

with observations $y_{i,x} \in \mathbb{N}_{\geq 0}$ and where $\lambda(x, U_i) = e^{U_i} g(x|\boldsymbol{\theta})$, U_i is a random effect variable with $E(U_i) = 0$ and $\text{Var}(U_i) = \sigma^2$ for $i = 1, 2, \ldots, n$ where n is the number of parents in the sample and $\text{Cov}(U_i, U_j) = 0$ for all $i \neq j$.

For this implementation, the likelihood function is then given by

$$\mathcal{L}(\boldsymbol{y}|\boldsymbol{\theta}, \sigma^2) = \left[\prod_{i=1}^{n}\left(\prod_{x\in E_i}\frac{\lambda(x, u_i)^{y_{i,x}}}{y_{i,x}!}e^{\lambda(x+1/2)}\right)f_U(u_i|\sigma^2)\right]. \tag{26}$$

3.2 Aggregated data

The most common type of data is aggregated as the number of females or males available to breed within a discrete age interval $[x, x+1)$ with observation vector $\mathbb{N}^\top = [n_0, n_1, \ldots, n_\omega]$ for the number of parents in the interval $[x, x+1)$. Here, following the model in Equation (21), we define the random variable $M_x = \sum_{i=1}^{n_x} Y_{i,x}$, where $T(x) = \sum_{j=0}^{x} M_j$ such that $\{T(x), x \geq 0\}$ is a compound Poisson process.

For aggregated data, the random variable of interest is then M_x. However, since $Y_{i,x}$ for $i \in I_x$ where I_x is an indexed set of individuals alive at age x are not identically distributed (ie, $Y_{i,x}|U_i \sim \text{Pois}[\lambda(x, U_i)]$) for all $i \in I_x$), the distribution of M_x needs to be fully specified. The resulting random variable is $M_x \sim \text{NB}(n_x\gamma, \gamma/[g(x)+\gamma])$, with probability mass function

$$f_M(m_x) = \frac{\Gamma(m+n\gamma)}{\Gamma(n\gamma)m!}\left(\frac{g(x)}{g(x)+\gamma}\right)^{m_x}\left(\frac{\gamma}{g(x)+\gamma}\right)^{n_x\gamma}, \quad \text{for } x \in \mathbb{N}_{\geq 0} \tag{27}$$

where $E[M_x] = n_x g(x)$ and $\text{Var}[M_x] = n_x g(x)[g(x)+\gamma]/\gamma$.

3.3 Individual level data with variable IBIs

The models in Equations (21) and (25) assume that all individuals alive at a given adult age x can potentially reproduce. This is an appropriate assumption when modeling the fertility of species with highly seasonal reproduction, IBIs of one-time units (eg, month, year), and when ages are measured at discrete intervals. However, for some populations or species, ages are recorded continuously, reproduction is continuous, and the time between reproductive events (ie, IBIs) may vary. In such cases, we might be interested in understanding age-specific fertility per reproductive event. Note then that the estimated age-specific fertility is no longer the average number of offspring produced by individuals in the discrete age interval $[x, x+1)$, $g_d(x)$, as in the previous 2 cases, but the average number of offspring produced per reproductive event of individuals of age x, namely $g_c(x)$.

Different processes lead to each reproductive event, several of which may not be fully revealed unless the proper information is available (Figure 3).

As I show in Figure 3, after reaching the minimum age at sexual maturity, α, individuals produce the first offspring after a specific time, which varies among individuals. Here, we can define a random variable, W, for the time to first birth after α, with realizations $w \geq 0$. Note that W can be a function of individual differences in maturation and fecundity.

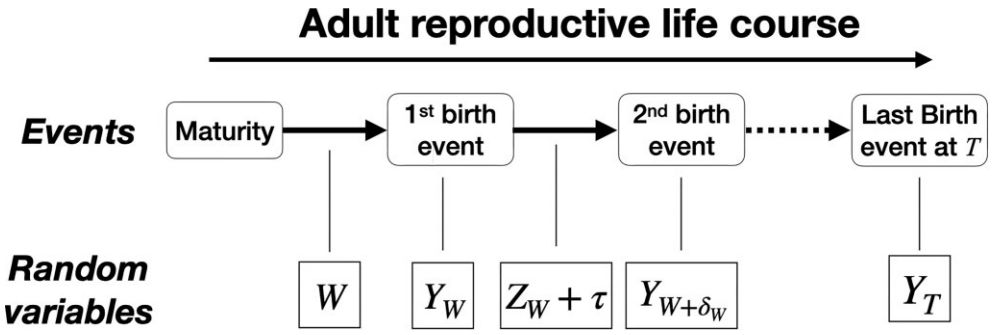

FIGURE 3 Schematic representation of the reproductive life course events and their associated random variables required for inference on age-specific fertility, time to first birth, and IBIs. The random variables are W for the time since maturity to first birth, Y_x for the number of offspring produced during the birth event at age x, and Z_x is the time between the last and current birth events (ie, IBI). Note that, for display purposes, the individual subscript i is not included.

After the first birth, each subsequent birth event will be a function of the individual's age, x, and the time since the last birth, namely the IBI (Susie Lee, 2022). Let Z_x be a random variable for the IBI; this is the time between the birth event at age x and the last birth event, with realizations $z_x \geq 0$. Note that IBIs include the gestation period and, depending on the species, the weaning age of the offspring from the previous birth event unless the offspring dies before reaching weaning age. In that case, the realizations are $z_x = \delta_x - \tau$ for $\delta_x \geq \tau$ where δ_x is the actual IBI, and τ is gestation time or the addition of weaning age and gestation time. At each birth event, the random variable $Y_{i,x}$ for the litter or clutch size of individuals i at age x is conditionally distributed as

$$\begin{aligned} Y_{i,x}|W \geq w_i \vee Z_x = z_{i,x} &\sim F_Y(y_{i,x}|\boldsymbol{\theta}, \gamma, w_i, z_{i,x}) \\ W_i &\sim F_W(w_i|\kappa) \\ Z_{i,x}|V_i &\sim F_{Z|V}(z_{i,x}|v_i, \eta) \\ V_i &\sim N(0, \sigma_v^2), \end{aligned} \tag{28}$$

where parameter γ accounts for individual variability in fertility, following the same implementation as in Equations (21) and (25). Variable V_i is a normally distributed random variable for individual random effects on IBI. Both, W_i and $Z_{i,x}$ are time to event random variables, and thus an exponential or similar time to event distributions are appropriate. For illustration purposes, let $W_i \sim \exp(\kappa)$ and $Z_{i,x}|V_i \sim \exp(\eta e^{v_i})$. The likelihood for individual i is given by

$$\mathcal{L}(\ldots) = \begin{cases} \gamma e^{-\gamma w_i} f_Y(y_{i,x}|\boldsymbol{\theta}, \gamma) & \text{for } x = w_i \\ \eta e^{-e^{v_i}\eta z_{i,x}} f_Y(y_{i,x}|\boldsymbol{\theta}, \gamma) & \text{for } x > w_i. \end{cases} \tag{29}$$

Importantly, this implementation requires precise knowledge of all reproductive events, including those that failed to produce offspring. If only successful births are known, then it is possible to use a zero-inflated conditional distribution for $Y_{i,x}$.

4 INFERENCE WITH THE R PACKAGE BAFTA

4.1 Basic setting

For inference, I constructed a Bayesian inference R package called BaFTA that facilitates making inferences on age-specific fertility for different types of data, that is, aggregated data, individual seasonal data (ie, discrete ages), and individual data with continuous ages and variable IBIs. The package, which allows testing the majority of the fertility models described in Section 2, uses Markov chain Monte Carlo (MCMC) with Metropolis–Hastings (Metropolis et al., 1953; Hastings, 1970) for the fertility and time to event parameters and direct sampling for the random effects standard deviations with gamma conjugate prior density.

For instance, the posterior for the model in Equation (28) used for the individual level data with continuous ages and variable IBI is

$$\begin{aligned} &p(\boldsymbol{\theta}, \alpha, \eta, \gamma, \sigma_v|\boldsymbol{y}, \boldsymbol{w}, \boldsymbol{z}) \\ &\quad \propto p(\boldsymbol{y}, \boldsymbol{w}, \boldsymbol{z}|\boldsymbol{\theta}, \gamma, \eta, \gamma, \sigma_v) p(\boldsymbol{\theta}|\boldsymbol{\mu}_\theta, \boldsymbol{\sigma}_\theta) p(\gamma|\mu_\gamma, \sigma_\alpha) \\ &\quad \times p(\eta|\mu_\eta, \sigma_\eta) p(\kappa|\mu_\kappa, \sigma_\kappa) p(\sigma_v|r_1, r_2), \end{aligned} \tag{30}$$

where the first term on the right-hand side of Equation (30) is the likelihood function as in Equation (29), while the following terms are prior densities for the parameters. For the other 2 types of datasets, the posterior is simplified accordingly.

The prior distribution for $\boldsymbol{\theta}$ is truncated normal with mean $\boldsymbol{\mu}_\theta$ and variance $\boldsymbol{\sigma}_\theta$, truncated at 0 for parameters with support on the positive real line, and at $-\infty$ for parameters in $\mathbb{R}$. Similarly, the prior distributions for γ, η, and κ are truncated normal with means μ_γ, μ_η, and μ_κ and variances σ_γ, σ_η, and σ_κ, all truncated at 0. Note that BaFTA sets default prior means and standard deviations, which can be modified by the user.

4.2 Accounting for missing or incomplete information

Given the difficulties of sampling in natural environments for ecological and evolutionary studies, it is often common that reproduction and fertility records are incomplete. For instance, some adult individuals that can produce offspring may be partially observed or undetected at a given sampling occasion. On the other hand, it is often difficult to know the ages of individuals that are first detected as adults, and therefore, their ages at each reproductive event or season are uncertain. To accommodate these sources of uncertainty, BaFTA extends inference to unknown ages and uncertain number of offspring produced per individual.

4.2.1 *Uncertain ages*

When the ages of some of the parents are unknown, the user should provide an estimated age at each birth occasion, while they should also provide the minimum and maximum possible ages for those individuals. For a given individual i with uncertain ages, let the vector of ages at offspring birth proposed by the user be $\boldsymbol{x}_i^{p\top} = [x_{i,1}^p, \ldots, x_{i,T}^p]$. Given the species minimum age (eg, minimum age at sexual maturity) α and maximum reproductive age ω, the sampling range for the uncertain ages is $\delta_i \in [L_i, U_i]$ such that $L_i = x_{i,1}^p - \alpha$ and $U_i = \omega - x_{i,T}^p$. Thus, for each age $x_{i,j}$ for $j = 1, \ldots, T$, the minimum sampling age is $x_{i,j} - L_i$ and the maximum sampling age is $x_{i,j} + U_i$, with resulting vectors of minimum and maximum ages $\boldsymbol{x}_i^L$ and $\boldsymbol{x}_i^U$.

At each iteration, BaFTA draws a random value δ_i^* from a truncated normal distribution $f(\delta, 0, 1, L_i, U_i)$ bound in the interval $[L_i, U_i]$ with mean 0 and variance 1. Thus, the new vector of ages are $\boldsymbol{x}_i^* = [x_{i,1}^*, \ldots, x_{i,T}^*]$ is $\boldsymbol{x}_i^* = \boldsymbol{x}_i + \delta_i^*$.

After sampling each age, BaFTA calculates the posterior for the vector of ages $\boldsymbol{x}_i^*$ as

$$p(\boldsymbol{x}_i^*|\boldsymbol{\theta}, \boldsymbol{y}_i, \boldsymbol{x}_i^p, \sigma_x^2, \boldsymbol{x}_i^L, \boldsymbol{x}_i^U) \propto p(\boldsymbol{y}_i|\boldsymbol{\theta}, \boldsymbol{x}_i^*) p(\boldsymbol{x}_i^*|\boldsymbol{x}_i^p, \sigma_x^2, \boldsymbol{x}_i^L, \boldsymbol{x}_i^U), \quad (31)$$

where the first term on the right-hand-side of Equation (31) is the likelihood function, $p(\boldsymbol{x}_i^*|\boldsymbol{x}_i^p, \sigma_x^2, \boldsymbol{x}_i^L, \boldsymbol{x}_i^U)$ is a truncated normal prior for the proposed ages, with mean vector given by the ages proposed by the user, $\boldsymbol{x}_i^p$ and variance σ_x^2 and truncated at $\boldsymbol{x}_i^L$ and $\boldsymbol{x}_i^U$. The variance is

$$\sigma_x^2 = \frac{1}{n_u} \sum_{i \in I_u} \frac{U_i - L_i}{2\ \Phi^{-1}(0.999)},$$

where n_u is the number of individuals with unknown age with indexed set I_u, and Φ^{-1} is the quantile function for the standard normal distribution. The value of σ_x^2 can be modify by the user if necessary, either as a single value, or as different values per record in case the uncertainty in the age estimates varies among individuals. Similarly, the user can modify the lower and upper bounds for the ages, for instance, if they are certain that a given individual cannot be younger or older than a given age.

BaFTA then uses Metropolis–Hastings to sample the proposed ages with acceptance probability

$$r = \min\left[1, \frac{p(\boldsymbol{x}_i^*|\ldots)}{p(\boldsymbol{x}_i)|\ldots)} \frac{f(0|\delta_i^*, 1, L_i, U_i)}{f(\delta_i^*|0, 1, L_i, U_i)}\right]. \quad (32)$$

Note that this procedure can be used on both individual data models.

4.2.2 *Uncertain number of offspring*

When parents are only partially followed during the reproductive season and the birth event is not witnessed, the number of offspring observed from those parents can, therefore, be a fraction of the number they produce. For instance, female chimpanzees often move away from their group when they are about to give birth and may not return until several weeks or even months later (Nishie and Nakamura, 2018). If the infant did not survive, then the observed number of offspring would be 0, although one was born. Similarly, for species that produce more than 1 offspring, if observers only follow the mother and its surviving infants after the birth event, only the alive fraction of the offspring will be detected.

The user can provide a variable representing the proportion of the reproductive season each of those parents was observed, when it does not include the birth event. Let $p_{i,t} \in [0, 1]$ be the proportion for parent i at reproductive season t. For individuals that were fully observed, we have that $p_{i,t} = 1$ while, for those that were partially observed, we have $p_{i,t} < 1$. For these records, the real number of offspring $y_{i,t}$ is treated as a latent variable to be estimated that is a function of the observed number of offspring, $o_{i,t}$ (ie, $o_{i,t} \leq y_{i,t}$). Let I_p be an indexed set of partially observed reproductive occasions. BaFTA estimates the number of offspring produced within the index I_p by drawing a random number of offspring per record, $y_{i,t}^*$ from a rounded truncated normal distribution, f, with mean given by the estimated number of offspring in the previous step, $y_{i,t}$, truncated at the lower bound at $o_{i,t}$ and with standard deviation 1. The prior for this proposed value uses a negative binomial PMF to evaluate the probability of the number of failures, that is, $y_{i,t}^* - o_{i,t}$ with mean given by

$$\mu_{i,t}^* = g(x_{i,t}|\boldsymbol{\mu}_\theta, \mu_\gamma)\ p_{i,t}, \quad (33)$$

and scale parameter μ_γ. Therefore, the posterior for each proposed number of offspring is

$$p(y_{i,t}^*|x_{i,t}, o_{i,t}, \ldots) \propto p(x_{i,t}|y_{i,t}^*, \boldsymbol{\theta}) p(y_{i,t}^* - o_{i,t}|\mu_{i,t}^*, p_{i,t}, \boldsymbol{\mu}_\theta, \mu_\gamma), \quad (34)$$

where the first term on the right-hand-side of Equation (34) is the likelihood as in Equation (24) and the second term is the negative binomial prior. BaFTA then uses Metropolis–Hastings to sample the proposed number of offspring with acceptance probability

$$r = \min\left[1, \frac{p(y_{i,t}^*|\ldots)}{p(y_{i,t})|\ldots)} \frac{f(y_{i,t}|y_{i,t}^*)}{f(y_{i,t}^*|y_{i,t})}\right]. \quad (35)$$

Note that this procedure can only be used on the individual level data with discrete ages.

4.3 Computation and diagnostics

The package uses parallel computing by means of the R package snowfall (Knaus, 2022) to run multiple MCMC chains. Potential scale reduction is calculated for each parameter to estimate convergence (Gelman et al., 2013). This diagnostic is calculated as $\hat{R} = \sqrt{\hat{v}^+/W}$, where W is a measure of the within-sequence variance and $\hat{v}^+$ is a weighted average of the between-sequence variance (B) and W. Convergence is attained when $\hat{R}$ is close to 1. As a rule of thumb, BaFTA uses an arbitrary upper bound of $\hat{R} < 1.05$ above which it assumes that parameters have not converged.

If all parameters have converged, BaFTA calculates deviance information criterion (DIC; Spiegelhalter et al., 2002). DIC approximates the expected predictive deviance as

$$\text{DIC} = 2\hat{D}_{avg}(y) - D_{\hat{\theta}}(y),$$

where y denotes the observed data, $\hat{D}_{avg}(y)$ is the mean discrepancy between the data and the model as a function of the parameters θ, averaged over the posterior distribution, while $D_{\hat{\theta}}(y)$

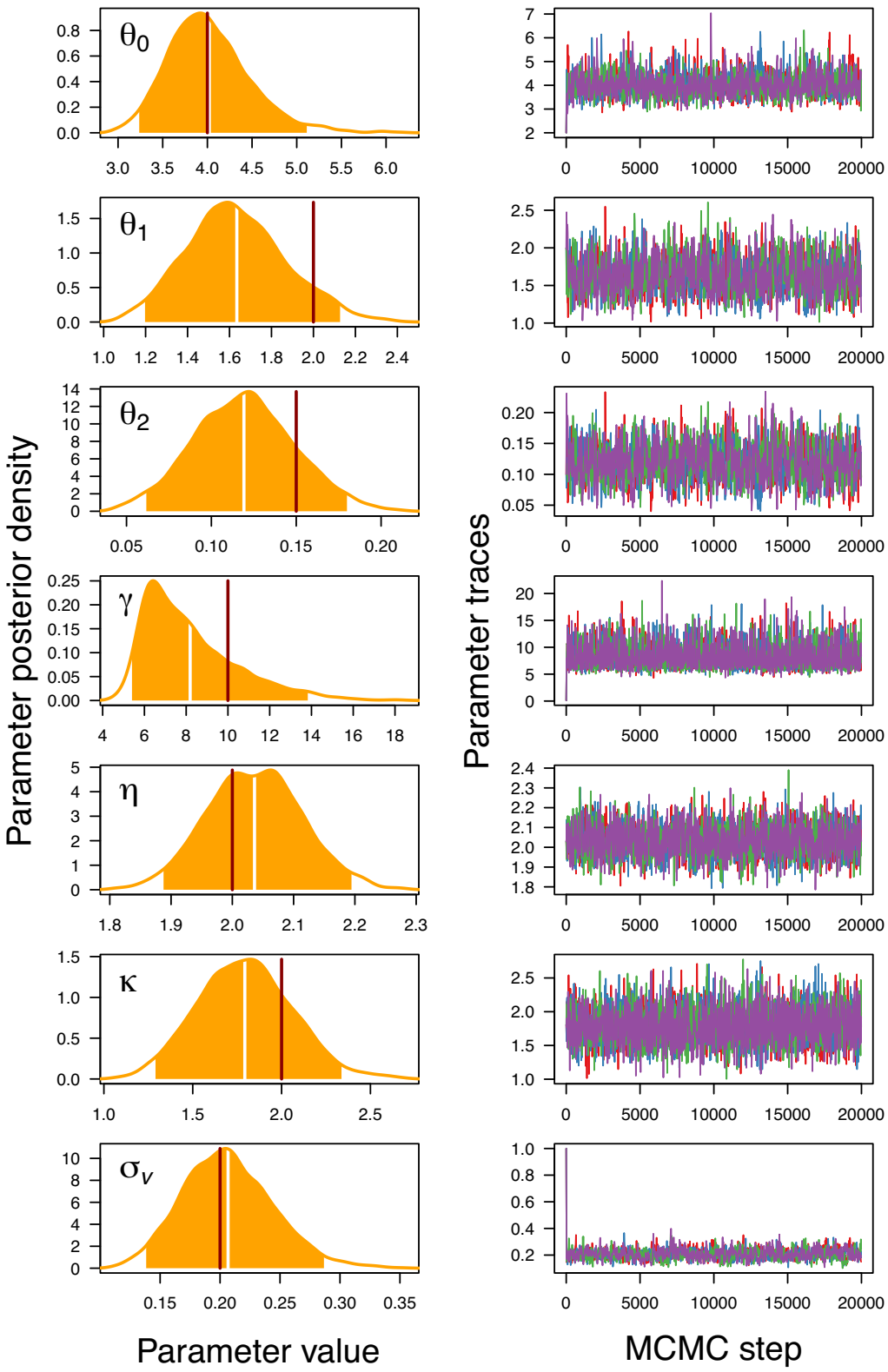

FIGURE 4 Plots of parameter posterior densities and traces from a BaFTA output with gamma model in Equation (8) applied to simulated data. The vertical dark lines show the parameters used for the simulation.

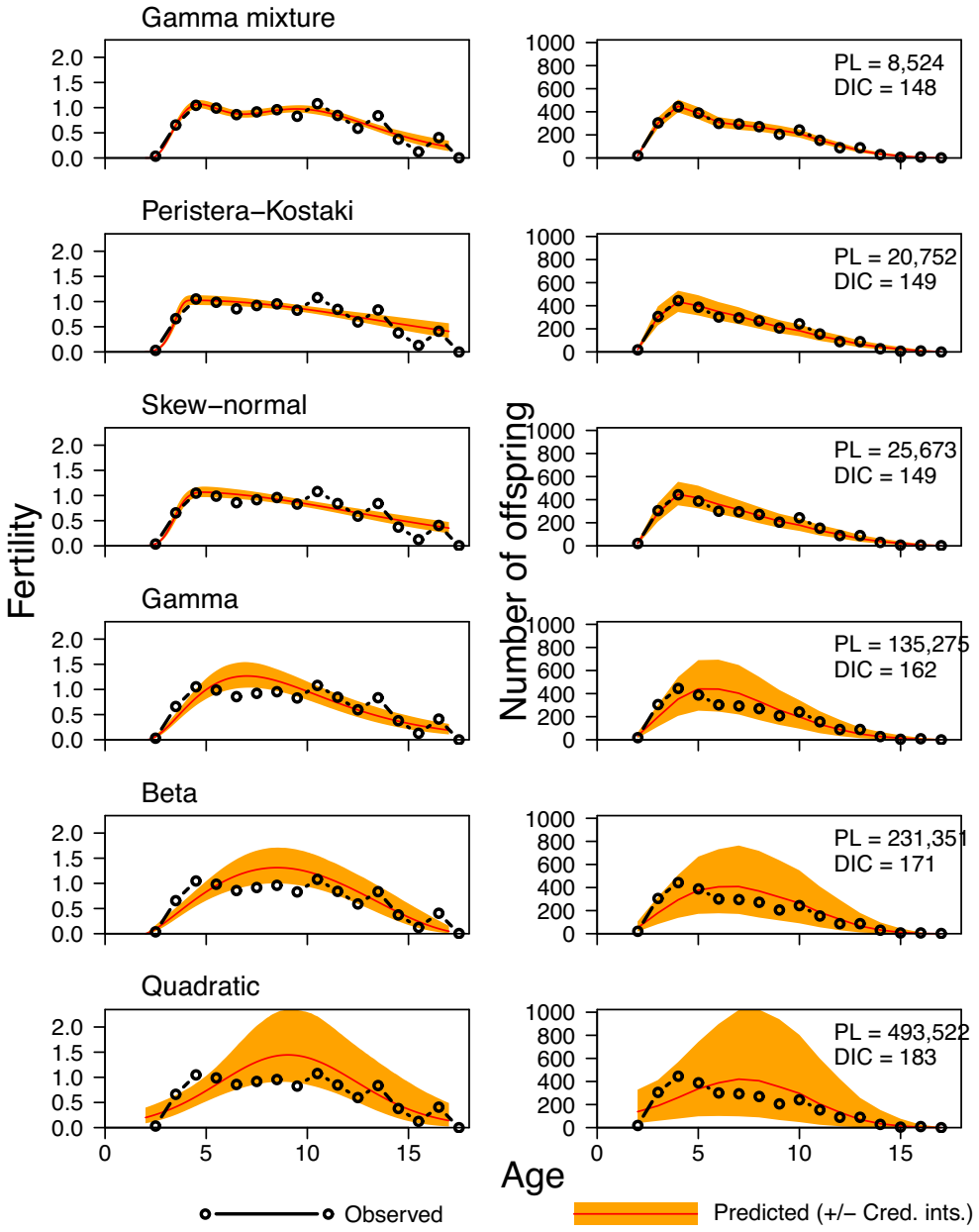

FIGURE 5 Inference on age-specific fertility for female lions (Packer et al., 1998) from aggregated data. The left panels show the observed and estimated fertility, this last including the 95% credible intervals, while the right panels show the observed and the predicted number of offspring produced per age, these last including the 95% predictive intervals. The models are sorted from lowest (top) to highest (bottom) predictive loss values (PL) (Gelfand and Ghosh, 1998). Inference was carried out with the R package BaFTA presented here.

is the discrepancy at the posterior mode (here represented by the point estimate $\hat{\theta}$). It is important to outline that the use of DICs is still controversial, and therefore, the results need to be taken with caution (see responses in Spiegelhalter et al., 2002). To improve the measure provided, BaFTA's DIC is calculated as an approximation to the group-marginalized DIC presented by Millar (2009). In addition, BaFTA calculates predictive loss as described by Gelfand and Ghosh (1998). This measure requires producing a vector of the predicted number of offspring $\hat{\boldsymbol{y}}|\boldsymbol{y}$, where $\boldsymbol{y}$ are the observed number of offspring. With these $\hat{\boldsymbol{y}}$ estimates we can construct a prediction distribution integrated across the posterior densities of the parameters as

$$p(\hat{\boldsymbol{y}}|\boldsymbol{y}) = \int \dots \int p(\hat{\boldsymbol{y}}|\boldsymbol{\theta})p(\boldsymbol{\theta}|\boldsymbol{y})d\theta_0 \dots d\theta_p. \quad (36)$$

The integrals in Equation (36) are evaluated numerically by means of the converged parameter traces, and the expected predictions are approximated as

$$E[\hat{\boldsymbol{y}}|\boldsymbol{y}] = \frac{1}{M}\sum_{m=1}^{M} E[\hat{\boldsymbol{y}}|\hat{\boldsymbol{\theta}}_m], \quad (37)$$

where M is the total number of MCMC iterations, and $\hat{\boldsymbol{\theta}}_m$ is the vector of parameters estimated at step m. Mean and upper and lower 95% predictive intervals are included as part of the BaFTA

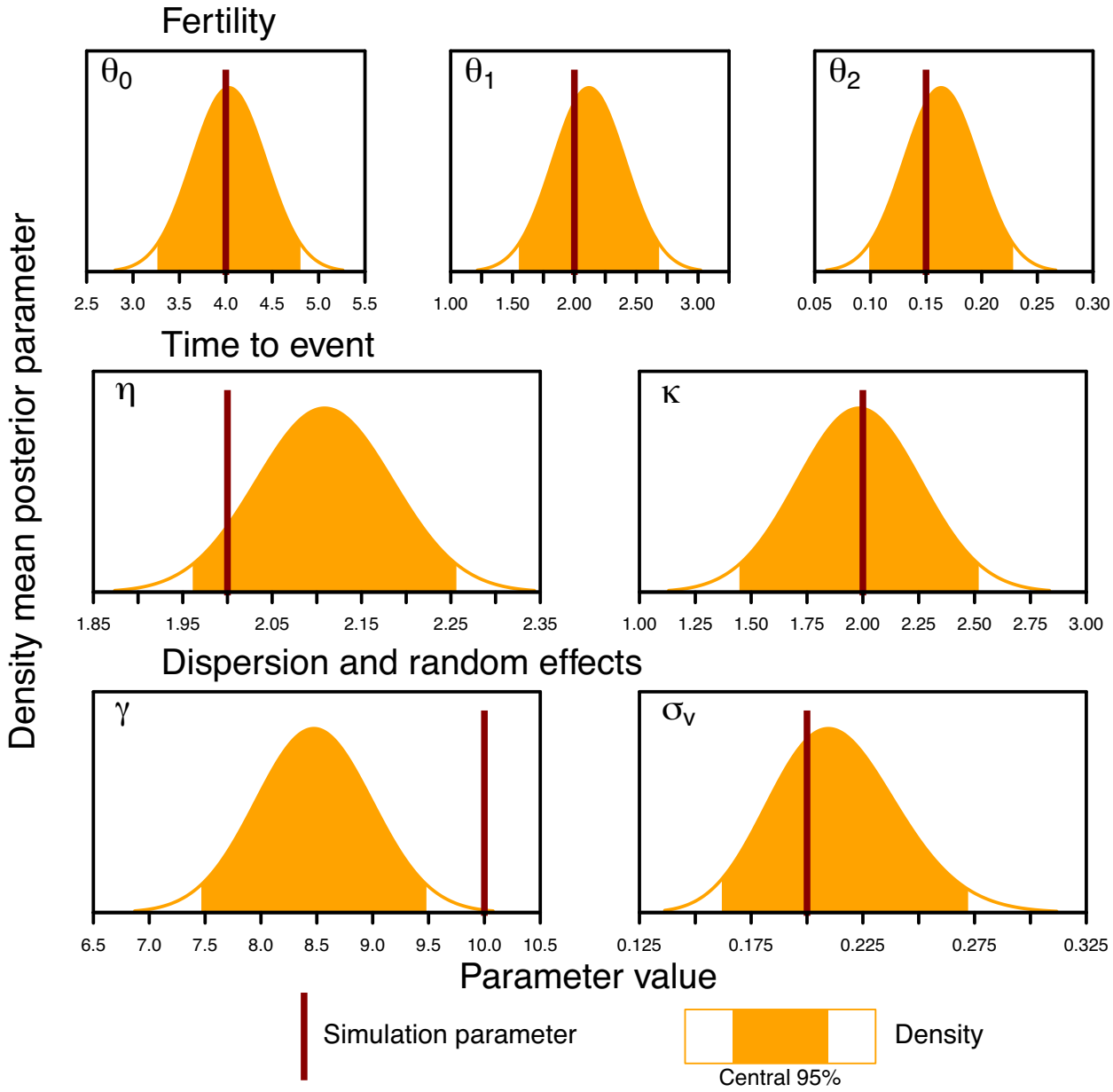

FIGURE 6 Simulation study of 1000 simulations selecting 100 parents, depicting the distributions of mean estimated parameter values (densities), calculated from the posterior densities from each simulation, and the parameters used for simulation (dark vertical lines). The fertility parameters correspond to the gamma distributional model in Equation (8).

output. With these, BaFTA calculates predictve loss, D, by first calculating a measure of goodness of fit

$$G = \sum_{i=1}^{N} (E[\hat{\boldsymbol{y}}|\boldsymbol{y}] - \boldsymbol{y})^2 \tag{38}$$

and a measure of model dispersion, or penalty term, given by the predictive variance

$$P = \sum Var[\hat{\boldsymbol{y}}|\boldsymbol{y}]. \tag{39}$$

Predictive loss is then calculated as $D = G + P$.

In Web Appendix A, I show the results of performance tests on MacOS and Linux platforms for the aggregated and individual-level data with variable IBI. I show that computing times are considerably fast, with low serial autocorrelation and good convergence. A visual inspection of the parameter posterior densities and traces demonstrates proper convergence in the model (Figure 4).

5 APPLICATIONS

5.1 Application on published aggregated data

The most common type of published data available is aggregated fertility records as described in Section 3.2. To illustrate the use of BaFTA on this type of data, I ran inference on age-specific fertility on the data provided by Packer et al. (1998)

for female African lions in the Serengeti National Park and Ngorongoro Crater, Tanzania. The data consists of the numbers of females and offspring born per age of the mothers. For this example, I tested 6 of the models available in BaFTA and ranked them based on their performance in terms of predictive loss. I show that the gamma mixture model performed best, followed by the Peristera–Kostaki (Figure 5).

In Web Appendix B, I provide a similar analysis on female olive baboon data from Gombe National Park, Tanzania (Packer et al., 1998) (Figures S1 and S2).

5.2 Simulation study

To illustrate how inference can be achieved under the implementations described Sections 3 and 4, I simulated a data set in which each individual life course followed the steps depicted in Figure 3 using the gamma fertility model in Equation (8) (see simulation details in Web Appendix C). With this data set, I ran 1000 simulations, sampling at random 100 reproducing individuals each time and sub-setting the complete reproduction data set (on average 850 reproductive events). I compared the quadratic and gamma models using DIC and predictive loss and recorded the number of simulations for which the "real" parameters used for simulation fell within the 95% credible intervals of the estimated parameters.

The simulation study results show that, even with as few as 100 reproducing individuals, the gamma model had the lowest predictive loss in 89.2% of cases, while it had the lowest DIC 92.8% of the times. Overall, almost all parameters were at least 96% of the times contained within the 95% credible intervals, except for β_0, which was within the 95% credible intervals 81.6% of the times. Most of the "real" parameters used for simulating the data fell within the 95% confidence intervals of the distributions of the posterior mean parameters. A notable exception was γ, the parameter responsible for over-dispersion in the negative binomial distribution (Figure 6). Although this may suggest some bias in its estimation, the "real" parameter was within the 95% of the credible intervals 99.8% of the times.

In Web Appendix C, I provide results for tests on discrete age data (Figures S3 and S4; Tables S4 and S5) and on aggregated data (Figures S4 and S5; Tables S6 and S7), where the results remained consistent with those from the continuous age data. I also ran tests on incomplete data, namely for simulations in which half of the individuals have unknown ages (Figures S6 and S7) and simulations where 25% of the number of offspring are uncertain (Figures S8 and S9). The results show that, for both types of missing data sources, the model retrieves appropriately the parameters used for simulation as well as the latent variables.

6 CONCLUSION

Despite the importance of age-specific fertility for ecological and evolutionary studies, the models used in these disciplines tend to be limited to a handful of simple, tractable, albeit, for the most part, unrealistic models. On the other hand, many alternative models have been developed in other disciplines, but the methods for inference do not appropriately apply to typical data sets in ecology and evolution. Nonetheless, as I hope to have demonstrated here, it is possible to use this vast array of age-specific fertility models by improving the inference methods to better account for the statistical needs of evolutionary and ecological data. By increasing the arsenal in our demographic toolkit with better and more appropriate tools, we can only improve our ability to understand the evolutionary and ecological processes we painstakingly work to unravel.

SUPPLEMENTARY MATERIALS

Supplementary material is available at *Biometrics* online.

Web Appendices referenced in Sections 4-5, along with R scripts and data to implement the proposed analyses in Sections 4-5, are available with this paper at the Biometrics website on Oxford Academic.

FUNDING

I thank the support from the eScience Center of the University of Southern Denmark (SDU) for allowing me to use their UCloud HPC platform.

CONFLICT OF INTEREST

None declared.

DATA AVAILABILITY

All data and code to reproduce the results in this paper are available in Zenodo at https://doi.org/10.5281/zenodo.15223647.

REFERENCES

Alberts, S. C., Altmann, J., Brockman, D. K., Cords, M., Fedigan, L. M., Pusey, A. et al. (2013). Reproductive aging patterns in primates reveal that humans are distinct. *Proceedings of The National Academy of Sciences of the United States of America*, 110, 13440–13445.

Asili, S., Rezaei, S. and Najjar, L. (2014). Using skew-logistic probability density function as a model for age-specific fertility rate pattern. *BioMed Research International*, 2014, 790294.

Azzalini, A. (1985). A class of distributions which includes the normal ones. *Scandinavian Journal of Statistics*, 2, 171–178.

Beer, J. d. (2011). A new relational method for smoothing and projecting age-specific fertility rates: TOPALS. *Demographic Research*, 24, 409–454.

Bermúdez, S., Blanquero, R., Hernández, J. A. and Planelles, J. (2012). A new parametric model for fitting fertility curves. *Population Studies (Cambridge)*, 66, 297–310.

Bradshaw, C. and McMahon, C. (2008). Fecundity. In: *Encyclopedia of Ecology, Population Dynamics*, 1535–1543. Amsterdam: Elsevier.

Brass, W. (1968). Note on Brass method of fertility estimation. *Brass, W.; Coale, AJ et al. The Demography of Tropical Africa, Part 1*, 140–142. Princeton, NJ: Princeton University Press.

Caswell, H. (2019). *Sensitivity Analysis: Matrix Methods in Demography and Ecology*. Cham: Springer Open.

Chandola, T., Coleman, D. A. and Hiorns, R. W. (1999). Recent European fertility patterns: Fitting curves to 'distorted' distributions. *Population Studies (Cambridge)*, 53, 317–329.

Clutton-Brock, T. H. and Isvaran, K. (2007). Sex differences in ageing in natural populations of vertebrates. *Proceedings. Biological Sciences/The Royal Society*, 274, 3097–3104.

Coale, A. J. and Trussell, T. J. (1974). Model fertility schedules: variations in the age structure of childbearing in human populations. *Population Index*, 44, 185–258.

Colchero, F., Eckardt, W. and Stoinski, T. (2021). Evidence of demographic buffering in an endangered great ape: Social buffering on immature survival and the role of refined sex-age classes on population growth rate. *Journal of Animal Ecology*, 90, 1701–1713.

Colchero, F., Jones, O. R., Conde, D. A., Hodgson, D., Zajitschek, F., Schmidt, B. R. et al. (2019). The diversity of population responses to environmental change. *Ecology Letters*, 22, 342–353.

Dugdale, H. L., Pope, L. C., Newman, C., Macdonald, D. W. and Burke, T. (2011). Age-specific breeding success in a wild mammalian population: selection, constraint, restraint and senescence. *Molecular Ecology*, 20, 3261–3274.

Ellis, S., Franks, D. W., Nattrass, S., Cant, M. A., Bradley, D. L., Giles, D. et al. (2018). Postreproductive lifespans are rare in mammals. *Ecology and Evolution*, 8, 2482–2494.

Gelfand, A. and Ghosh, S. (1998). Model choice: a minimum posterior predictive loss approach. *Biometrika*, 85, 1–11.

Gelman, A., Carlin, J. B., Stern, H. S., Dunson, D. B., Vehtari, A. and Rubin, D. B. (2013). *Bayesian Data Analysis. Chapman and Hall/CRC*. 3rd edn. Boca Raton: Chapman and Hall/CRC.

Gupta, A. and Pasupuleti, S. S. R. (2013). A new behavioural model for fertility schedules. *Journal of Applied Statistics*, 40, 1–10.

Hadwiger, H. (1940). Eine analytische reproduktionssunktion für biologische gesamtheiten. *Scandinavian Actuarial Journal*, 1940, 101–113.

Hastings, W. K. (1970). Monte Carlo sampling methods using Markov chains and their applications. *Biometrika*, 57, 97–109.

Hoem, J. M., Madien, D., Nielsen, J. L., Ohlsen, E.-M., Hansen, H. O. and Rennermalm, B. (1981). Experiments in modelling recent Danish fertility curves. *Demography*, 18, 231–244.

Islam, R. (2011). Modeling of age specific fertility rates of Jakarta in Indonesia: a polynomial model approach. *International Journal of Scientific and Engineering Research*, 2, 1–5.

Knaus, J. (2022). *Snowfall: Easier Cluster Computing (Based on 'snow')*. R package version 1.84-6.2. Available at: https://CRAN.R-project.org/package=snowfall[Accessed 17 December 2024].

Lemaître, J.-F., Ronget, V. and Gaillard, J.-M. (2020). Female reproductive senescence across mammals: a high diversity of patterns modulated by life history and mating traits. *Mechanisms of Ageing and Development*, 192, 111377.

Levitis, D. A. and Lackey, L. B. (2011). A measure for describing and comparing postreproductive life span as a population trait. *Methods in Ecology and Evolution*, 2, 446–453.

Lowe, W. H., Kovach, R. P. and Allendorf, F. W. (2017). Population genetics and demography unite ecology and evolution. *Trends in Ecology and Evolution*, 32, 141–152.

Ma, Y. and Genton, M. G. (2004). Flexible class of skew-symmetric distributions. *Scandinavian Journal of Statistics*, 31, 459–468.

Mazzuco, S. and Scarpa, B. (2011). Fitting age-specific fertility rates by a skew-symmetric probability density function. Technical report, University of Padua.

Mazzuco, S. and Scarpa, B. (2015). Fitting age-specific fertility rates by a flexible generalized skew normal probability density function. *Journal of the Royal Statistical Society: Series A (Statistics in Society)*, 178, 187–203.

McCleery, R. H., Perrins, C. M., Sheldon, B. C. and Charmantier, A. (2008). Age-specific reproduction in a long-lived species: the combined effects of senescence and individual quality. *Proceedings. Biological Sciences/The Royal Society*, 275, 963–970.

Metropolis, N., Rosenbluth, A. W., Rosenbluth, M. N., Teller, A. H. and Teller, E. (1953). Equation of state calculations by fast computing machines. *Journal of Chemical Physics*, 21, 1087–1092.

Millar, R. B. (2009). Comparison of hierarchical Bayesian models for overdispersed count data using DIC and Bayes' factors. *Biometrics*, 65, 962–969.

Muller, M. N., Blurton-Jones, N. G., Colchero, F., Thompson, M. E., Enigk, D. K., Feldblum, J. T. et al. (2020). Sexual dimorphism in chimpanzee (Pan troglodytes schweinfurthii) and human age-specific fertility. *Journal of Human Evolution*, 144, 102795.

Nishie, H. and Nakamura, M. (2018). A newborn infant chimpanzee snatched and cannibalized immediately after birth: Implications for "maternity leave" in wild chimpanzee. *American Journal of Physical Anthropology*, 165, 194–199.

Packer, C., Tatar, M. and Collins, A. (1998). Reproductive cessation in female mammals. *Nature*, 392, 807–811.

Peristera, P. and Kostaki, A. (2007). Modeling fertility in modern populations. *Demographic Research*, 16, 141–194.

Schmertmann, C. (2003). A system of model fertility schedules with graphically intuitive parameters. *Demographic Research*, 9, 81–110.

Sharp, S. P. and Clutton-Brock, T. H. (2010). Reproductive senescence in a cooperatively breeding mammal. *Journal of Animal Ecology*, 79, 176–183.

Spiegelhalter, D., Best, N., Carlin, B. and Linde, A. V. D. (2002). Bayesian measures of model complexity and fit. *Journal Of The Royal Statistical Society Series B—Statistical Methodology*, 64, 583–639.

Susie Lee, D. (2022). Interbirth interval. In: *Encyclopedia of Animal Cognition and Behavior*, 3622–3624. Cham: Springer.

Received: January 18, 2024; Revised: May 2, 2025; Accepted: June 12, 2025